Structural Vibration for Robotic Communication and Sensing on One-Dimensional Structures

Maxwell Hill[1], Jerry Mekdara[2], Barry Trimmer[2] and Robert White[1]

***Abstract*— In this paper, structure-borne vibrations in a one-dimensional structure are examined as a means of communication and sensing for networks of robots. The concept is inspired by the observation that insects may use structural vibrations to communicate and to detect features of their environment. A 12 x 5 x 6 cm mobile robot capable of traversing an acoustically favorable structure is presented. A technique for measuring distance between robots and communicating commands to robots using vibrations generated on a common one-dimensional substrate are presented, and demonstrated through preliminary experimental results. Design considerations for this type of system are also discussed.**

I. INTRODUCTION

Creatures in nature transmit and receive information at high speeds using structure-borne vibration. This *mechanocommunication* is direct in the sense that the transmitted information is generated by another creatures movement, and the received signal is a sensory response to this action. In fact, 70 % of insect species may use substrate vibration of some form to communicate [1].

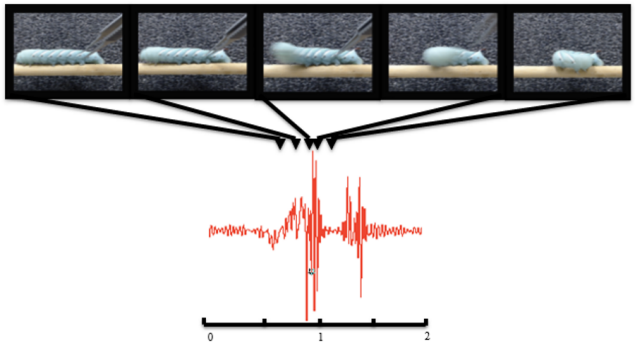

Fig. 1. *Manduca sexta* caterpillar on a wooden dowel exhibiting a strike reflex (top) and the resultant transverse vibration at the substrate (bottom).

Many species of caterpillar communicate by producing and responding to sounds and substrate vibrations [2], [3]. Although *Manduca* caterpillars do not live in communities, they do produce trains of clicks (3 s trains, dominant frequency around 30 kHz) as part of their defensive behavior [4]. A vibratory response generated by striking behavior is illustrated in Fig. 1.

*This work was supported by the National Science Foundation

[1]Maxwell Hill and Robert White are with the Department of Mechanical Engineering, Tufts University, Medford, MA 02155, USA lloyd.hill@tufts.edu and r.white@tufts.edu

[2]Jerry Mekdara and Barry Trimmer are with the Department of Biology, Tufts University, Medford, MA 02155, USA prasong.mekdara@tufts.edu and barry.trimmer@tufts.edu

Some species can discriminate substrate vibrations produced by abiotic influences (rain, wind), conspecifics, and predators [5], [6]. A recent phylogenetic and morphological study suggested that ritualized vibratory signals (produced by anal scraping) originated from walking behavior [7]. One possibility, not yet explored, is that, before vibration detection was used for active communication, it evolved for evaluating the mechanical properties of the environment. Surface texture, stiffness and slip can all be detected through oscillations in shear force (vibrations) [8], [9].

A vibration communication and sensing system is proposed for mobile robots. This system would have advantages over RF communication in situations of limited spectrum and signal interference. The scheme is also covert in that it only allows communication between devices on the same substrate; devices close to the system cannot listen if they are mechanically isolated from the structure.

In addition to communication, vibrations can be used to sense properties of the environment. Interactions of the vibrations with branch points or terminal points in a structure, resulting in reflections, could allow the robot to generate local maps of the structure on which it is traveling.

One dimensional branching structures such as cables, structural trusses, pipes, and tracks, as well as natural structures like trees, are of particular interest for this application. These types of structures are very common in both nature and in human construction, and are important environments for robots tasked with inspection, material transportation, and surveillance tasks. These structures can support various modes of vibration including bending, torsional, and longitudinal vibrations [10]. Due to the one-dimensional nature of the structure, vibrations do not spread geometrically, potentially allowing for long range communication and sensing. The dispersive nature of bending waves in the vibrating structure can be exploited to give additional information about the environment that might not be available for non-dispersive waves such as longitudinal pressure waves.

Little prior work has been done on the use of structural vibrations for communication and sensing in robotics. In one instance, surface waves were used successfully for communication between robots on a common plate substrate using cross-correlation methods [11]. However, due to the two-dimensional substrate, this system lends itself only to close-proximity distributed communication methods because the vibrations die out quickly due to both geometric spreading and absorption. Localization was also achieved by measuring the variation of Time of Arrival (TOA) at each leg of a six-legged scorpion robot with similar range limitations [12].

A similar strategy, Time Delay of Arrival (TDOA), was implemented for a microphone array mounted on a robot for localizing sound [13]. Microphones are also used in recent work in tactile sensing skins for robots utilizes sensor node networks embedded in a flexible substrate to localize objects and characterize textures [14].

In another piece of prior work, acoustic reflectometry was used to remotely map complex tunnel networks, detecting distances to turns, turn types, and closures [15]. This application has more similarities to the method proposed here; the one dimensional nature of the acoustic medium allows the signal to propagate over long distances with losses caused only by absorption.

In this work, we begin to develop the necessary platforms and techniques to explore sensing and communication with structural vibrations for robots operating on one-dimensional substrates.

II. ROBOTIC PLATFORM AND ENVIRONMENT

A. Robotic Platform

A robotic platform was developed to traverse a track environment and to sense vibration propagated through the rails. A four-wheeled design was chosen, with the two front wheels driven by small geared motors, as shown in Fig. 2. Like wheels on a train, grooves in the wheels maintain alignment between the wheels and rails. In order to negotiate turns, the robot is split into two symmetric segments; which are pinned about an axis and give it a single degree of freedom.

The angle, θ, of one segment relative to the other, is sensed directly using a potentiometer. A Texas Instruments EZ430-RF2500 target board controls the robot via an integrated MSP430F2274 microcontroller. This microcontroller includes eight 10-bit ADC inputs which can be used for monitoring sensors. Currently, the potentiometer is the only sensor input. A CC2500 2.4GHz radio is also included on this board for wireless data-logging. A 7.4V 850mAh lithium polymer battery pack allows the robot to operate untethered.

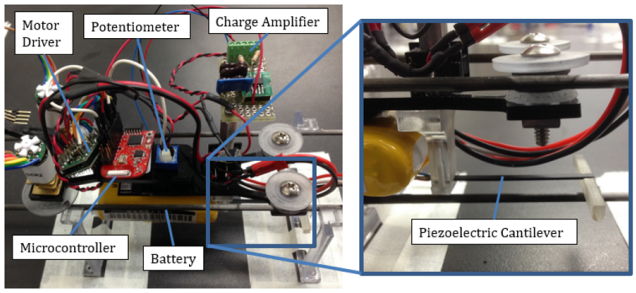

Fig. 2. The placement of components on the robot (left) and an illustration of the kinematics of the robot (right).

Closed-loop control of the robot was needed for the robot to traverse the track smoothly. A compressive preload in the beams connecting to the wheels maintains grip between the wheels and the rails. The kinematics of the robot governs a maximum angle at which the preload is insufficient to provide reliable motion. Therefore, a PID control loop was wrapped around θ. In designing the PID controller, Ziegler-Nichols tuning rules were used as a starting point.

The controller has two states: PID and an open-loop turning mode. Switching between these states is initiated when the robot hits a turn and causes to exceed a threshold. An interrupt then exits the PID loop for a single cycle of the turning mode control. For more complex track topologies with forked junctions, a similar strategy can be implemented. Instead of sensing the turns through angle, the junction features would be sensed via vibration and the robot will decide which way to turn and steer itself appropriately.

Piezoelectric bimorph cantilevers (PiezoDrive BA4902) serve as vibration transceivers. These cantilevers are ideal for this application because they can be configured both as an actuator or sensor, have high sensitivity, and kilohertz bandwidth. Similar elements were successfully used to detect vibration in a robot scorpion [13].

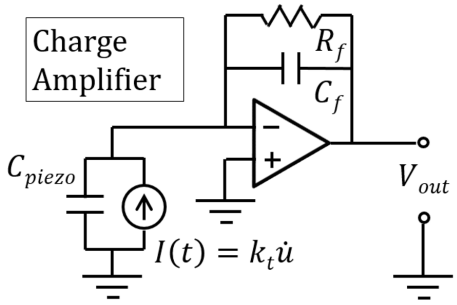

Fig. 3. Charge amplifier circuit used to condition piezoelectric cantilever sensor output.

To configure the cantilevers as actuators, a voltage amplifier (PiezoDrive PDu100B) steps up the on-board battery voltage up to 100 V to induce significant strain in the cantilevers. The amplifier operates over a nominal bandwidth of 3.2 kHz at 100 V, which is sufficient for preliminary investigation of communication and sensing schemes. For sensing, a charge amplifier circuit was constructed based on a transimpedance amplifier (current-to-voltage converter) topology, for measuring deflection of the piezoelectric cantilevers. A schematic of the charge amplifier is shown in Fig. 3.

B. Environment

In order to study vibration as a means of communication and sensing, an environment with low energy loss through damping was needed. Additionally, the structure needed to be simple enough for a robot to traverse robustly. A track structure was decided on with three carbon fiber rails; two of the rails are for the robot to attach to and one rail allowing vibration transmission. In order to test the robots mobility, the track was constructed in the shape of a closed loop, with the ability to add branches later (Fig. 4). The turn segments were 3D-printed from Stratsys VeroClear-RGD810 material and bonded to the straight carbon fiber segments with Loctite

Super Glue. The structure is 60 x 30cm in dimension, with four constant-radius 90 degree turns.

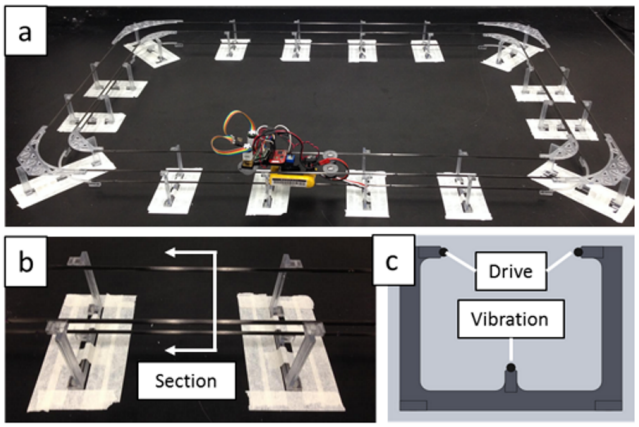

Fig. 4. Robot navigating track (a), a close-up of the three-rail structure (b), and a section view along the track (c).

III. MODELING

Before extending vibration communication and sensing methods to a robotic platform, modeling was needed to predict how vibrations propagate through the structure, and find any limitations. To reduce the problem, a single straight segment of the structure (Fig. 4) was investigated. In the model, two piezoelectric cantilevers are included; one cantilever provides a forcing to the structure and a second (at another location) senses structural vibration. These cantilevers represent the transducers on a pair of robots. A steady-state model was created from the loading configuration shown in Fig. 5.

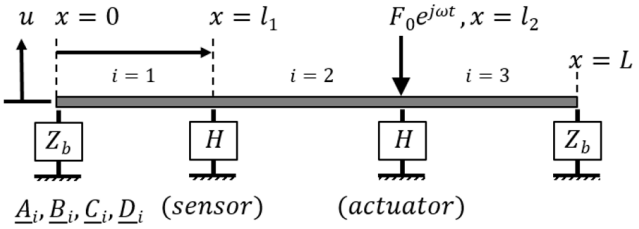

Fig. 5. Beam model loading configuration with boundary conditions.

The dynamic Euler-Bernoulli equation for beams was used as the basis of the model. This model is typically used for slender bending beams with no axial tension or compression [16].

$$EI\frac{\partial^4 u}{\partial x^4} + \rho A\frac{\partial^2 u}{\partial t^2} = 0 \tag{1}$$

Here, $u(x,t)$ is the transverse displacement, EI is the bending stiffness, and ρA is the mass per unit length. Arbitrary mechanical termination impedances are prescribed at the boundaries $x = 0$ and $x = L$, giving rise to four boundary conditions,

at $x = 0$

$$M|_{x=0} = EI\frac{\partial^2 u}{\partial x^2}\bigg|_{x=0} = Z_\theta \frac{\partial u}{\partial x}\bigg|_{x=0} \tag{2}$$

$$V|_{x=0} = EI\frac{\partial^3 u}{\partial x^3}\bigg|_{x=0} = Z_t u|_{x=0} \tag{3}$$

and at $x = L$

$$M|_{x=L} = EI\frac{\partial^2 u}{\partial x^2}\bigg|_{x=L} = Z_\theta \frac{\partial u}{\partial x}\bigg|_{x=L} \tag{4}$$

$$V|_{x=L} = EI\frac{\partial^3 u}{\partial x^3}\bigg|_{x=L} = Z_t u|_{x=L} \tag{5}$$

The cantilevers discussed in section II can be modeled as a simple mass-spring system as depicted in Fig. 6, where $H = \frac{m_e\omega^2 - k_e}{j\omega}$ is the mechanical impedance of the cantilever.

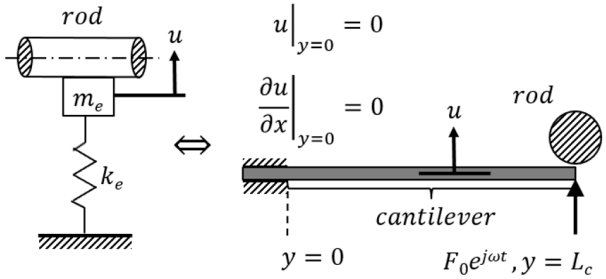

Fig. 6. Piezoelectric cantilever modeled as mass-spring system.

The values of m_e and k_e are determined by calculating the first mode of the cantilever,

$$\Omega_1 = 0.5969\pi \tag{6}$$

$$\omega_1 = \sqrt{\frac{EI}{\rho A}}\frac{\Omega_1^2}{L^2} \tag{7}$$

$$k_e = \frac{Ewh^3}{4L^3} \tag{8}$$

$$m_e = \frac{k_e}{\omega_1^2} \tag{9}$$

The input oscillation of the actuator, described as a harmonic force of magnitude F_0 at $x = l_2$ generates a force balance condition,

$$V|_{x=l_1,left} + V|_{x=l_1,right} = -Hj\omega\, \underline{u}|_{x=l_1} \tag{10}$$

and a similar condition at the sensor location $x = l_1$

$$V|_{x=l_2,left} + V|_{x=l_2,right} = -Hj\omega\, \underline{u}|_{x=l_2} + F_0 e^{j\omega t} \tag{11}$$

Six more boundary conditions arise by prescribing continuity of displacements, angles, and moments over the boundaries at $x = l_1$ and $x = l_2$,

$$u|_{x=l_1,left} = u|_{x=l_1,right} \tag{12}$$

$$\left.\frac{\partial u}{\partial x}\right|_{x=l_1,left} = \left.\frac{\partial u}{\partial x}\right|_{x=l_1,right} \tag{13}$$

$$\left.\frac{\partial^2 u}{\partial x^2}\right|_{x=l_1,left} = \left.\frac{\partial^2 u}{\partial x^2}\right|_{x=l_1,right} \tag{14}$$

$$u|_{x=l_2,left} = u|_{x=l_2,right} \tag{15}$$

$$\left.\frac{\partial u}{\partial x}\right|_{x=l_2,left} = \left.\frac{\partial u}{\partial x}\right|_{x=l_2,right} \tag{16}$$

$$\left.\frac{\partial^2 u}{\partial x^2}\right|_{x=l_2,left} = \left.\frac{\partial^2 u}{\partial x^2}\right|_{x=l_2,right} \tag{17}$$

For steady-state response at a single frequency we expect the solution to (1) to be of the following form, with two traveling waves (A and B) and two evanescent waves (C and D),

$$\underline{u}_i(x,t) = \underline{A}_i e^{j(\omega t - kx)} + \underline{B}_i e^{j(\omega t + kx)} + \underline{C}_i e^{j\omega t} e^{kx} + \underline{D}_i e^{j\omega t} e^{-kx} \tag{18}$$

where the wavenumber comes from the solution of the characteristic equation for the governing ODE,

$$k = \sqrt{\omega}\left(\frac{EI}{\rho A}\right)^{1/4} \tag{19}$$

It should be noted for bending waves that the wavenumber is proportional to the square root of frequency. This is equivalent to saying the wave speed for this dispersive wave is not constant; it varies inversely as the square root of frequency. This means that waveforms transmitted from one position will arrive with a different shape due to frequency dependent phase delays. Hence, typical methods used with RF and acoustic waves will not be optimal for use with dispersive waves such as structural bending.

The equations created by the twelve boundary conditions can be written in matrix form and solved for the coefficients through matrix inversion. Time is implicit in this steady-state model. The solutions arrived at are steady state, harmonic solutions. For finite structures with little damping, these steady state vibrations are quickly established. This is also an important feature of this type of substrate which differs from the typical mental model we may have of vibrations traveling out and away from a source in large spaces or spaces with considerable damping. Rather, vibrational energy is trapped in the one dimensional structure and quickly establishes a steady state vibration pattern which must be interpreted as such for communication and sensing.

Linearity of the governing equation ensures that multiple solutions at different drive frequencies may be superimposed. Depending on the impedances at the ends of the beam, different behaviors are observed. These behaviors range from pure standing waves to pure traveling waves, depending on how well the impedance boundary conditions are matched to the characteristic impedance for the bending wave.

Electromechanical coupling was also considered in this model. A coupling constant k_t relating the tip velocity of the piezoelectric cantilever to input current was derived [17]. For the first mode of the cantilever,

$$k_t = \frac{-3d_{31}Ebh}{4L} \tag{20}$$

where d_{31} is a piezoelectric constant; E is the modulus; and b, h, L are geometric parameters. The current through the cantilever is described as a function of k_t, as shown in Fig. 3 above. Similarly, the amplitude of the force generated by the cantilever and exerted onto the beam is expressed as $F_0 = k_t V_{app}$. The voltage amplifier is linear with a known gain.

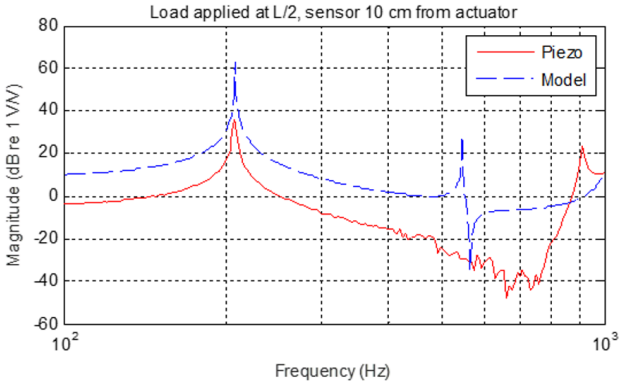

Fig. 7. Comparison of experiment and model prediction of sine-sweep of the piezoelectric sensor.

The model was validated by measuring the frequency response for physical embodiment of the model. In Fig. 7 we see the prediction captures the shape of the measured frequency response well. All parameters in the model are textbook properties and have not been tuned. The 13 dB lower signal level seen in experiment as compared to the model is under investigation. More importantly, this result shows that in this frequency range the dynamics of the cantilever dominate those of the beam, which is an important consideration for the design of communication and sensing schemes.

IV. COMMUNICATION AND SENSING

One salient quantity to measure in the context of robot networks is the distance between robot agents. We take this problem as an example of how steady state standing waves in a dispersive structure might be used to sense position. The method considered for this calculation examines phase change of an oscillation measured at a distance from the input. Here, phase refers to discrete regimes; the response is either in-phase or out-of-phase with the input.

In this scheme, a vibration is induced at a point along a beam and the response at any point on the beam can be referenced to this driving vibration to obtain a phase. In a

standing wave regime of a single frequency, the phase toggles between zero (in-phase) and 180 degrees (out-of-phase) at wave nodes. If the phase is interpreted as a binary code, for two drive frequencies, this gives a 2-bit output with position resolution determined by the half wavelength of the shortest wave.

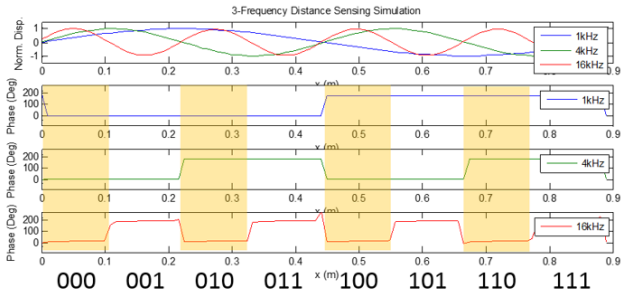

Fig. 8. Simulated beam response to three harmonic excitations (1 kHz, 4 kHz, and 16 kHz) (top) and the resulting phase interpreted as a three bit distance code (bottom).

Additional frequency components can be superimposed to increase spatial resolution. Doing so improves the resolution of the distance measurement from 2-bit to N-bit

$$R = \lambda_0 / 2^N \tag{21}$$

where N is the number of frequency components used and λ_0 is the wavelength of the lowest frequency (in Fig. 8 N=3 and $\lambda_0 = 0.9$ m). Each subsequent frequency selected should be four times the previous frequency in order to halve the wavelength, due to the square root nature of the wavenumber in equation (19). This relationship affects the required system bandwidth as

$$BW = f_0(4^{(N-1)} - 1) \tag{22}$$

where f_0 is the lowest frequency component. For this particular example, for a 90 cm long structure, three frequency components result in a spatial resolution of 11cm/bit. It is easy to imagine a signal with eight frequency components, which would achieve 0.35 cm/bit. The bandwidth growth with N, described in equation (22), does present a limitation on the number of frequency components. It is noted that f_0 need not be selected as a fundamental frequency, potentially shifting f_0 to a more tractable (lower) frequency for implementation in hardware. Nonetheless, bandwidth should be considered when selecting a vibration source and sampling rate.

Some preliminary testing has been completed to demonstrate the phase-shift distance measurement technique. For this testing, a rectangular acrylic specimen was used, as shown in Fig. 9. Acrylic has a stiffness of around 2 GPa, as compared to 10 GPa for carbon fiber. The estimated fundamental frequencies for a short segment are therefore reduced and are feasible for a bench-top experiment.

A laser doppler velocimeter (LDV) mounted on a micro-positioning stage was used to scan the length of the beam

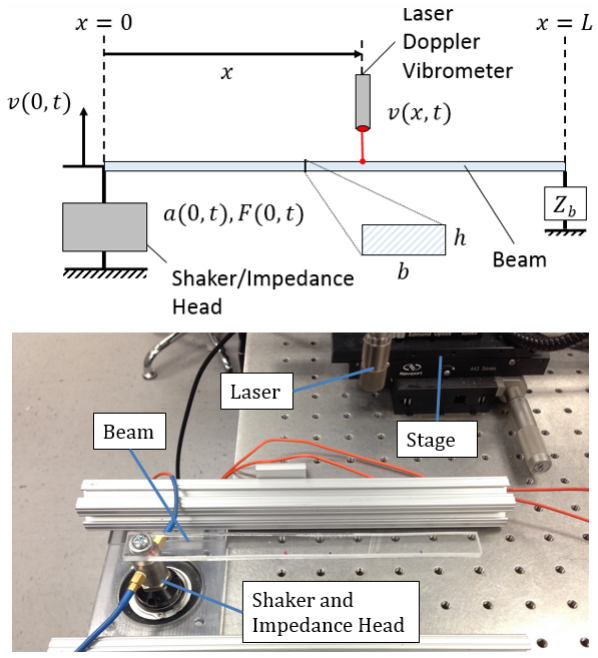

Fig. 9. Experimental setup for phase-shift method: schematic (top) and physical test setup (bottom). Note: for this case of a cantilever beam $Z_b = 0$.

and record vertical velocities as a result of two driving frequencies. These results were referenced to the acceleration measured directly at the shaker ($x = 0$) by an impedance head accelerometer, as shown in Fig. 9. Magnitude and phase data as a function of position was recovered from these measurements.

The experimental results shown in Fig. 10 demonstrate that the phase technique can be used to measure distance. The proposed model was used to estimate the harmonics of the chosen beam. Two frequencies of excitation were used to clearly distinguish four distinct regions of the beam. Some near-field effects can be seen close to the shaker ($x = 0$), where loading conditions do not entirely align with the idealized conditions of the model.

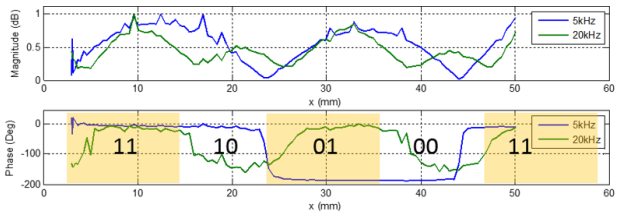

Fig. 10. Acryllic beam magnitude and phase response to 5 kHz and 20 kHz excitations.

This concept can be extended to a simple hypothetical pair of mobile robots, A and B, attached to a common beam. The vibration source is replaced with an actuator mounted to robot A and the LDV is replaced by a vibration sensor fixed to robot B some distance away. In order for the robots to calculate phase, a carrier vibration signal will also be needed to provide a common phase reference.

Further, a scheme for transmitting commands over vibration has been demonstrated on this robotic platform. The robot 'listens' for a burst (sinusoid at a uniform frequency) generated by a piezoelectric cantilever mounted to the track. Depending on the duration of the detected burst, the robot executes a distinct motor command, illustrated experimentally in Fig. 11.

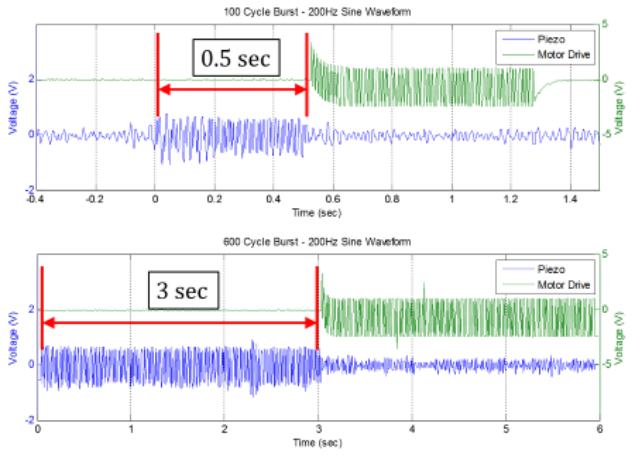

Fig. 11. The robot measures a 100 cycle burst and responds by executing a short (0.5 sec) drive command (top), while a 600 cycle burst triggers a longer (3 sec) drive command. Both bursts are at 200 Hz.

The robot behavior (motor drive signal) is recorded to demonstrates that the robot can distinguish discrete commands by looking only at properties of received structural vibration. While this demonstration shows one-directional communication, it can easily be extended to pairs of robots with the ability to both actuate and sense vibration, for two-way communication.

V. CONCLUSION

Structural vibrations are used by insects to communicate and sense information about their environment. This use of vibration may also be useful for mobile robots, particularly if operating on one dimensional branched structures such as cables, structural trusses, tracks, piping systems or natural structures such as trees. The method is particularly interesting in one-dimensional structures, since vibrations can propagate over long distances without the attenuation associated with geometric spreading that would occur in two and three dimensional spaces.

In this work we described a mobile robotic platform on a track that will be used to explore practical methodologies for the use of structure borne vibration in communication and sensing. We have demonstrated the ability to send simple commands to a mobile robot using structure borne vibration. An example methodology for distance sensing employing multi-frequency standing waves in a bending beam was demonstrated in a physics-based model and in experiment.

In future work we intend to explore the use of multiple robots agents on this platform. Additional communication schemes can be developed, employing FFT techniques to distinguish transmissions from multiple robots transmitting at distinct carrier frequencies. We also plan to test the limitations (range, resolution, and bandwidth) of the proposed distance-sensing scheme.

ACKNOWLEDGMENT

This research was supported in part by the National Science Foundation grants, IOS-1050908 to Barry Trimmer, IGERT-1144591 to Barry Trimmer and David Kaplan, and DBI-1126382 to Robert White.

REFERENCES

[1] R. Matthews, J. Matthews, Insect Behavior. Dordrecht, The Netherlands: Springer Netherlands, 2010, pp. 291-339.
[2] Yack, J., M. Smith, and P. Weatherhead, Caterpillar talk: acoustically mediated territoriality in larval Lepidoptera. Proceedings of the National Academy of Sciences, 2001. 98(20): p. 11371-11375.
[3] Yack, J.E., S. Gill, C. Drummond-Main, and T.N. Sherratt, Residency Duration and Shelter Quality Influence Vibratory Signalling Displays in A Territorial Caterpillar. Ethology, 2014. 120(4): p. 354-364.
[4] Bura, V.L., A.K. Hnain, J.N. Hick, and J.E. Yack, Defensive sound production in the tobacco hornworm, Manduca sexta (Bombycoidea: Sphingidae). Journal of insect Behavior, 2012. 25(2): p. 114-126.
[5] Guedes, R., S. Matheson, B. Frei, M. Smith, and J. Yack, Vibration detection and discrimination in the masked birch caterpillar (Drepana arcuata). Journal of Comparative Physiology A, 2012. 198(5): p. 325-335.
[6] Castellanos, I. and P. Barbosa, Evaluation of predation risk by a caterpillar using substrate-borne vibrations. Animal Behaviour, 2006. 72(2): p. 461-469.
[7] Scott, J.L., A.Y. Kawahara, J.H. Skevington, S.-H. Yen, A. Sami, M.L. Smith, and J.E. Yack, The evolutionary origins of ritualized acoustic signals in caterpillars. Nature communications, 2010. 1: p. 4.
[8] Greenleaf, J.F., M. Fatemi, and M. Insana, Selected methods for imaging elastic properties of biological tissues. Annual Review of Biomedical Engineering, 2003. 5(1): p. 57-78.
[9] Tiwana, M.I., S.J. Redmond, and N.H. Lovell, A review of tactile sensing technologies with applications in biomedical engineering. Sensors and Actuators A: Physical, 2012. 179(0): p. 17-31.
[10] Johnson, K.O., The roles and functions of cutaneous mechanoreceptors. Current opinion in Neurobiology, 2001. 11(4): p. 455-461.
[11] Silvola, Ari, Russell, Robin. Australian Robotics and Automation Assoc; 2005. Robot communication via substrate vibrations.
[12] Wallander, A., Russell, R.A., and Hyyppa, K., 'A robot scorpion using ground vibrations for navigation', Proceedings of the Australian Conference on Robotics and Automation, Melbourne, Aug 30- Sept 1, 2000, pp. 75-79.
[13] J. Valin, F. Michaud, J. Rouat, D. Letourneau, "Robust Sound Source Localization Using a Microphone Array on a Mobile Robot." IEEE/RSJ International Conference on Intelligent Robots and Systems, 2004.
[14] D. Hughes, N. Correll, 'A Soft, Amorphous Skin that can Sense and Localize Textures', IEEE International Conference on Robotics and Automation, 2014.
[15] Bowen, David. Development of a portable system for acoustical reconstruction of tunnel and cave geometries. J. Acoust. Soc. Am. 129, 2514 (2011).
[16] Inman, D. J. Engineering Vibration. 4th ed. Upper Saddle River, NJ: Pearson/Prentice Hall, 2014. 532-44. Print.
[17] Weinberg, Marc S. "Working equations for piezoelectric actuators and sensors." Microelectromechanical Systems, Journal of 8.4 (1999): 529-533.